

ARTICLES

Nonequilibrium hard-disk packings with controlled orientational order

Anuraag R. Kansal and Thomas M. Truskett

*Department of Chemical Engineering, Princeton University, Princeton, New Jersey 08544*Salvatore Torquato^{a)}*Department of Chemistry and Princeton Materials Institute, Princeton, New Jersey 08544*

(Received 4 November 1999; accepted 26 June 2000)

This paper addresses one of the fundamental questions in the theory of hard-disk packings—how order within a system relates to packing density. The algorithm presented is a seed-based, growth protocol in which new disks are added sequentially to the surface of a growing cluster. The angular position of the new disk is chosen based on the minimization of an objective function designed to control order, as measured by the global bond-orientational order parameter ψ_6 , which varies between 0 and 1 (with 1 indicating perfect hexagonal close-packed order). Modifying the objective function allows the final packing fraction to be biased while maintaining tight control over ψ_6 . Inside of the range $0 \leq \psi_6 \leq 0.70$, the targeted order parameter ψ_6 is achieved to within two decimal places of accuracy. Furthermore, it is found that random structures ($\psi_6 \sim 0.01$) can be generated with packing fractions in the range $0.40 \leq \eta \leq 0.77$. Interestingly, the algorithm can produce nonequilibrium hard-disk configurations that are considerably more disordered than those typical of the equilibrium fluid. © 2000 American Institute of Physics. [S0021-9606(00)50436-X]

I. INTRODUCTION

The systematic investigation of hard-sphere packings by computer simulation has a long history, which finds its roots in the theory of liquids and glasses (see, e.g., Refs. 1–5). In view of the mathematical richness of the sphere-packing problem and the wide variety of related applications in the physical and biological sciences (e.g., colloidal systems,⁶ granular materials⁷ and biological membranes⁸), it is surprising that many basic questions remain unanswered, such as: What is the relationship between the degree of order in a system and its density? How does the nature of this relationship depend on the protocol used to generate the sphere packings? These questions are fundamental to understanding the statistical geometry of condensed-phase systems⁹ and have recently led to a reassessment of the random close-packed state for spheres.¹⁰ In the present work, we address the related question: How does the degree of order within a system affect the range of densities the system can attain?

The study of close-packed random systems is a problem of great interest.^{11–18} Early investigators, such as Adams and Matheson,¹⁴ discovered that growth algorithms that rely on the random addition of contacting spheres produce densities that are noticeably lower than those measured in experimental random packings.^{15,16} To address this issue, Adams and Matheson (and independently Bennett¹⁷) developed new growth protocols that were deterministic in nature. In the method of Adams and Matheson, a core or seed of several close-packed spheres was placed at the origin. Then particles

were added sequentially to the point closest to the origin such that the new spheres established contact with three existing spheres in the cluster. In a similar fashion, Bennett developed two distinct criteria for sequential addition of particles to the growing seed. The first rule, coined the “global” criterion, is identical to that of Adams and Matheson. A second criterion, termed the “local” criterion, prescribes that the particles be added sequentially to the three-contact pockets in which the added particle is closest to the plane of its three nearest neighbors. Both criteria produce systems that appear random, but suffer from noticeable shortcomings. For instance, the configurations generated by these protocols do not reproduce the characteristic split-second peak in the radial distribution function (RDF) observed in the experimental packings. Furthermore, the resulting structures are highly anisotropic.

In commonly used protocols for generating dense configurations of spheres, such as those mentioned above, a predetermined packing prescription is followed that is expected to generate random structures.^{2,14,17,18} The resulting configurations can then be checked for signatures of long-range order and the packing fraction can be measured. In this paper, a new serial addition protocol is introduced in which *the degree of order is controlled throughout the formation of the packing*. In other words, as each disk is added to the existing cluster, its placement is chosen so as to minimize an objective function designed to prescribe the degree of bond-orientational order in the system. In addition, modifications which allow the packing fraction to be biased, while retaining tight control over the degree of order in the system, are

^{a)} Author to whom correspondence should be addressed.

included. Our attention is restricted to the two dimensional hard-disk system in this work; however, the methodology can be readily generalized to hard spheres in three dimensions.

The use of a serial algorithm allows the bond-orientational order to be varied using a single parameter—the position of the disk being placed. Implementing a similar algorithm for an N -particle system would require a function with $6N$ terms (corresponding to the number of bonds in the system) to be optimized. In addition, in such an algorithm, maintaining a highly coordinated system would be very difficult, thereby likely reducing the maximum densities attainable. Finally, we have found that when placing spheres in contact with one another in series, the translational order created is very short ranged (see Discussion), and the bond-orientational order can be varied independently of it, allowing the effects of bond-orientational order to be considered alone.

Order in systems of identical spheres in d spatial dimensions can take the form of translational or bond-orientational order. The importance of the different types of order can be readily seen in theories that describe the melting of hard-disk crystals. In the proposed hexatic phase (of the KTHNY theory), disks possess only short-ranged translational order, while exhibiting long-ranged orientational order.^{19–22} Translational order can be investigated through the familiar radial distribution function, $g(r)$, which is the inverse Fourier transform of the static structure factor $S(k)$ (obtained from scattering experiments). Bond-orientational order, at the simplest level, may be characterized by a single order parameter. In two dimensions, the global bond-orientational order parameter ψ_6 , may be defined as

$$\psi_6 = \left| \frac{1}{N_{\text{bond}}} \sum_j \sum_k e^{6i\theta_{jk}} \right|, \quad (1)$$

where j runs over all disks in the system, k runs over all neighbors of disk j , θ_{jk} is the angle between some fixed reference axis in the system and the bond connecting the centers of disks j and k , and N_{bond} is the total number of such bonds in the system.^{20,21} In the present work, the reference axis is chosen to be the positive x -axis, but this choice is completely arbitrary. The neighbors in this study are “geometric neighbors,” which can be formally determined using the Delaunay tessellation.²³ The order parameter ψ_6 measures the coherence of sixfold symmetry in the system, which is characteristic of the hexagonal closed-packed state (HCP) in two dimensions. For a perfect HCP lattice, $\psi_6 = 1$, while $\psi_6 \sim N_{\text{bond}}^{-1/2}$ for an ideal gas.

The protocol presented here packs a fixed area, subject to periodic boundary conditions, with monodisperse disks. In what we term the *basic algorithm*, the packing fraction η is entirely determined by the prescribed value of ψ_6 [in two dimensions, $\eta = N\pi\sigma^2/(4A)$, where σ is the hard-disk diameter, N the number of disks, and A is the system area]. However, it is found that the packing fractions resulting from the basic algorithm ($\eta \approx 0.67$ at low ψ_6 values) are substantially lower than those typically considered to be in the random close-packed state in two dimensions ($\eta_{\text{RCP}} \approx 0.81$).² To test how high the packing fraction can be driven while

retaining control over ψ_6 , a biasing parameter, a , has been introduced. Likewise, a second biasing parameter α_{ex} has also been included to create packing fractions substantially lower than those that result from the basic algorithm.

Section II describes the algorithm and associated parameters in detail. In Sec. III, the properties of the structures generated using the algorithm are analyzed. Finally, Sec. IV discusses some related packings as well as some useful extensions to the algorithm.

II. METHODS

As noted in the Introduction, the protocol can be best understood as a basic algorithm in which packings are formed with the control of orientational order being the only consideration. Two parameters are then added which allow a bias in the final packing fraction. The description contained here will adhere to the following format: first we describe the basic algorithm, and then we consider modifications that allow a greater range of packing fractions to be generated with a specified degree of orientational order.

A. Basic algorithm

The algorithm is a serial growth protocol, beginning with a seed and depositing additional disks one at a time to the surface of the cluster. Periodic boundary conditions are enforced on the square simulation box. Most of the simulations are carried out in a $26\sigma \times 26\sigma$ box, allowing the deposition of roughly 550–650 disks per configuration, where it is recalled that σ is the hard-disk diameter. To test the effect of system size, runs were also performed in boxes four to nine times as large in area. The algorithm is initiated by the placement of a small seed containing several disks. We have found the results to be largely independent of the structure of this initial seed. For the results presented here, the seed consisted of three disks in a close-packed triangular arrangement. Each new disk is deposited and fixed in place so that it is in contact with at least one existing disk in the cluster. The process terminates when no more space is available for disks to be deposited.

To determine where a new disk cannot be added, a list of “locked” host disks is maintained. This list comprises all existing disks which do not have room for a new disk to be placed in contact with them without overlap. When the list contains all particles, the system is locked and the process is terminated. However, while potentially unlocked disks remain in the system, one of these disks is chosen randomly and the new disk will be placed in contact with that disk, if possible.

Once a host disk is chosen for placement of a new disk, the program identifies all the other disks within 2σ of the center of the host disk. These disks are termed “limiting” disks and represent the particles which may overlap the newly placed disk. The limiting disks are then sorted by the angles formed between the bond connecting the limiting disk to the host disk and the reference axis. This creates a set of potential gaps between pairs of limiting disks inside of which the new disk may be placed. Beginning from a randomly chosen gap, each subsequent gap is checked in turn until one

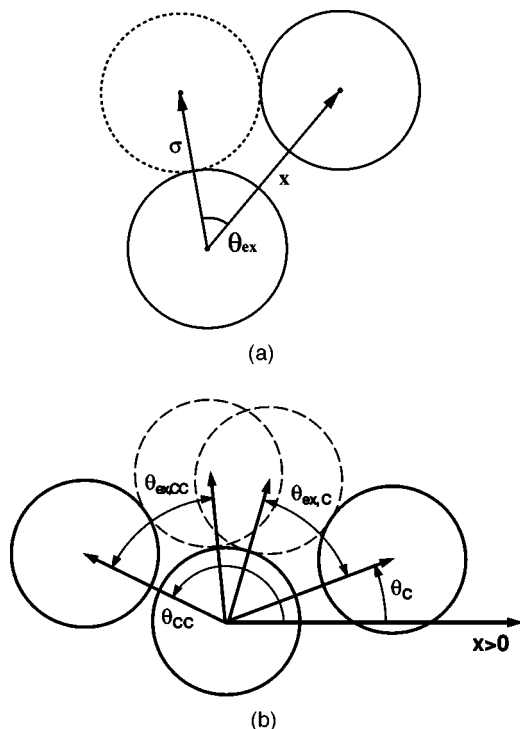


FIG. 1. (a) Schematic demonstrating the angle θ_{ex} excluded by a limiting disk. The new disk (broken circle) is placed in contact with the host disk (at the vertex) as closely as possible to the limiting disk. (b) Illustration of a gap between two limiting disks (solid circles). In this case, space is available and a new disk may be placed between the two broken circles, i.e., at any angle θ that satisfies the relation $\theta_C + \theta_{\text{ex},C} \leq \theta \leq \theta_{\text{CC}} - \theta_{\text{ex},\text{CC}}$.

is found that has enough space to contain the new disk. This check is facilitated by defining an “exclusion angle” θ_{ex} , which is the minimum value of the angle connecting the centers of a new disk, the host disk (at the vertex), and the limiting disk, which avoids overlap between the new disk and the limiting disk. This quantity is illustrated in Fig. 1(a). The exclusion angle θ_{ex} is calculated as

$$\theta_{\text{ex}} = \cos^{-1} \left(\frac{x}{2\sigma} \right), \quad (2)$$

where x is the distance between the host disk and the limiting disk. The criterion for determining whether available space exists within a gap is then equivalent to asking if there exists some angular position θ such that

$$\theta_C + \theta_{\text{ex},C} \leq \theta \leq \theta_{\text{CC}} - \theta_{\text{ex},\text{CC}}, \quad (3)$$

where θ_C is the angular position of the limiting disk in the clockwise direction, $\theta_{\text{ex},C}$ is the exclusion angle associated with this disk, and θ_{CC} and $\theta_{\text{ex},\text{CC}}$ are the analogous quantities for the limiting disk in the counterclockwise direction. If this inequality holds, then a new disk may be placed in the gap between these two limiting disks. This is illustrated schematically in Fig. 1(b). If, however, no gaps are found which allow for placement of the new disk, then the host disk is moved to the “locked” list and a new host disk is chosen.

Once a gap with sufficient room for a new disk has been identified, the angular placement of the new disk can be determined. The new disk may be placed at any angular posi-

tion θ which obeys relation (3). The algorithm then selects the value of θ that minimizes the objective function, Φ , which is defined as

$$\Phi = |\psi_6 - \psi_{6,\text{target}}|, \quad (4)$$

where ψ_6 is the global orientational-order parameter for the system of disks [Eq. (1)] including the new disk, and $\psi_{6,\text{target}}$ is the desired value of the order parameter.

Here, it is appropriate to briefly discuss the method for calculating the orientational order parameter. It has generally been found that global ψ_6 is insensitive to the definition for “neighboring disks.”²⁴ A popular definition for neighbors of a given disk is the set of disk centers that lie within some maximum distance of that disk, which is very inexpensive computationally. In the algorithm described in this paper, however, this choice leads to undesirable results. In particular, the inclusion (or exclusion) of one additional disk generally has a dramatic effect on the orientational order parameter. As such, it is found that new disks will be preferentially placed with neighbors that are just within the specified maximum neighbor distance, introducing artificial translational order into the structure generated. To avoid this problem, neighbor disks in this algorithm are chosen to be the “geometric neighbors” as defined by the Delaunay triangulation.²³ The Delaunay lattice is the dual of the Voronoi tessellation. In the Voronoi tessellation, each site (defined by a disk center in the present context) is assigned the region of space closer to it than to any other site. This tiles the plane into polygons. Then Delaunay triangulation can then be generated by connecting those sites whose associated Voronoi polygons share a common edge.

The procedure used in the current algorithm to find the optimal position for the newly added disk is relatively simple. The possible range of values for θ is divided into several evenly spaced trial positions. The global orientational-order parameter ψ_6 is then calculated for the system, with the disk located in each trial position in turn. A new pair of bounds surrounding the best trial position is then set and the process is repeated several times. This iterative method has some weaknesses that are important to note. Calculating the global ψ_6 value is computationally expensive. This cost is reduced to some degree by using the iterative search method. The use of iterations, however, means that it is possible that the first sweep will find a local, rather than the global, minimum. To reduce this possibility, more trial locations can be tested, but this results in a proportional increase in computational time. Here, it is simply noted that when implemented, this method is sufficient to produce ψ_6 values very close to those targeted, and it seems to afford a good compromise between performance and programming simplicity.

B. Algorithm enhancements

The basic algorithm allows impressive control over the value of the global orientational order parameter, but no independent control over the packing fraction of the system. In order to generate a more diverse range of configurations, two small modifications have been made to the algorithm which allow greater influence over the packing fraction. The first is

the inclusion of an additional term in the objective function in Eq. (4). The modified objective function, Φ_{mod} , is

$$\Phi_{\text{mod}} = |\psi_6 - \psi_{6,\text{target}}| + a|\theta - \theta_{\text{lim}}|, \quad (5)$$

where

$$\theta_{\text{lim}} = \begin{cases} \theta_C + \theta_{\text{ex},C} & |\theta - (\theta_C + \theta_{\text{ex},C})| \leq |\theta - (\theta_{CC} - \theta_{\text{ex},CC})| \\ \theta_{CC} - \theta_{\text{ex},CC} & |\theta - (\theta_C + \theta_{\text{ex},C})| > |\theta - (\theta_{CC} - \theta_{\text{ex},CC})| \end{cases} \quad (6)$$

and θ represents the trial angular position of the new disk. The additional term in the modified objective function favors placing a disk closer to its limiting positions. This tends to create local structures that are *more closely packed*, and thereby biases the overall packing fraction towards higher values. It is important to note that the parameter a is defined to be non-negative. We have found that negative values of a do not produce lower density structures.

Instead, to produce a bias towards lower densities (as compared to the basic algorithm), a third parameter α_{ex} is included (along with $\psi_{6,\text{target}}$ and a). This parameter serves to increase the effective exclusion angle around disks, θ_{mod} , according to

$$\theta_{\text{mod}} = \theta_{\text{ex}} + \alpha_{\text{ex}}. \quad (7)$$

This new exclusion angle then changes the criterion that allows a disk to be placed [given in Eq. (3)] to

$$\theta_C + \theta_{\text{mod},C} \leq \theta \leq \theta_{CC} - \theta_{\text{mod},CC}, \quad (8)$$

where $\theta_{\text{mod},C}$ and $\theta_{\text{mod},CC}$ are the effective exclusion angles around the clockwise and counterclockwise neighbors, respectively. This change prevents a disk from being placed in a small gap, where it otherwise might have fit. Like a , α_{ex} must be non-negative. A negative value would allow overlaps to occur. In passing we note that if $\alpha_{\text{ex}} > \pi/6$, then any given disk can be placed in contact with only two other disks (which would result in the formation of undesirable chain-like structures). Thus, α_{ex} is effectively bounded from above.

The total computer time required for generating a single configuration varies considerably with system size. A system of $N = 600$ disks requires approximately 11 min to run on an IBM SP2 node. The CPU time scales roughly as N^2 . Appreciable room for improvement in execution time exists in both the optimization routine and the calculation of the Delaunay triangulation.

III. RESULTS

Individual configurations for trials with different parameter sets are shown in Fig. 2. In particular, Fig. 2(a) shows what may be considered a baseline configuration, in which $\psi_{6,\text{target}} = a = \alpha_{\text{ex}} = 0$. In other words, orientational order is minimized without biasing the packing fraction. Figure 2(b) depicts a configuration in which $a = \alpha_{\text{ex}} = 0$, but $\psi_{6,\text{target}}$ is raised to 0.5. This represents a moderately ordered system in which the packing fraction is still not biased. In Fig. 2(c), $\psi_{6,\text{target}}$ and α_{ex} are again set to a zero, but $a = 0.01$, i.e., minimizing order and simultaneously biasing towards higher packing fraction. Finally, Fig. 2(d) shows a system in which $\psi_{6,\text{target}} = a = 0$ and $\alpha_{\text{ex}} = \pi/15$, i.e., minimizing order again, but now biasing towards low packing fraction.

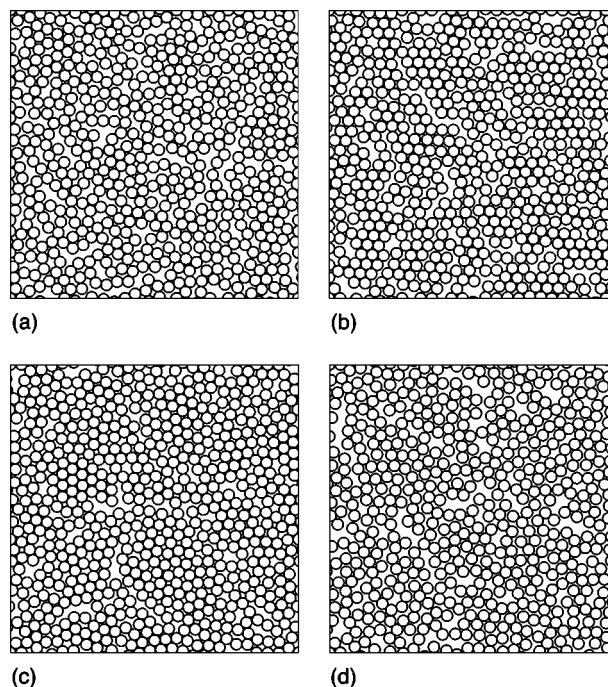


FIG. 2. Single configurations generated using four different parameter sets. (a) $\psi_6 = 0.004$, $\eta = 0.674$, (b) $\psi_6 = 0.497$, $\eta = 0.708$, (c) $\psi_6 = 0.004$, $\eta = 0.745$, (d) $\psi_6 = 0.005$, $\eta = 0.633$. A description of the parameters used in generating these configurations is contained within the text.

Visual inspection of these configurations allows for a few important observations to be made. First, note the absence of appreciable HCP order in the structures (a) and (d). This stands in stark contrast to the random close-packed configurations of disks reported elsewhere,^{2,25} which show significant orientational ordering. Furthermore, some insight into the nature of ψ_6 can be gained by comparing Figs. 2(a) and 2(c). In both of these configurations, the global order parameter ψ_6 is very low (roughly 0.004). However Fig. 2(a) appears to be more disordered by inspection. This points out one of the important limitations of the global quantity ψ_6 as a measure of order in a system. The global measurement cannot account for the formation of small pockets of local order which are randomly oriented relative to one another. Finally, note the appearance of long, thin voids in all of the configurations. These voids may be considered in analogy to the bridge structures present in granular materials. It has been shown previously that such structures are the result of collective reorganizations in the granular material⁷ and as such their appearance in our sequential addition algorithm is interesting. Voids drive down the packing fraction and understanding their origin may suggest a method for creating even denser structures. However, the collapse of bridge structures has been shown to produce small ordered clusters, suggesting that eliminating the voids in our packings may promote localized regions of high order.²⁶

Overall, the algorithm provides excellent control over orientational order for a substantial range of the parameters. Table I summarizes the ψ_6 values obtained for three sets of the parameters. First, notice that all three of the parameter sets shown in Table I have some maximum limit of $\psi_{6,\text{target}}$, above which the actual ψ_6 value begins to diverge from the

TABLE I. Comparison of ψ_6 values achieved using various parameter sets. The results listed are averages over between 20 and 100 configurations.

$\psi_{6,\text{target}}$	$a=0$		$a=0.01$		$a=0$	
	$\alpha_{\text{ex}}=0$		$\alpha_{\text{ex}}=0$		$\alpha_{\text{ex}}\approx 0.21$	
0	0.0024	± 0.0018	0.0048	± 0.0028	0.0045	± 0.0022
0.1	0.0997	± 0.0019	0.0988	± 0.0043	0.0986	± 0.0060
0.2	0.1990	± 0.0020	0.1995	± 0.0041	0.1879	± 0.0092
0.3	0.2989	± 0.0022	0.2964	± 0.0042	0.2302	± 0.0238
0.4	0.3990	± 0.0022	0.3973	± 0.0054		
0.5	0.4977	± 0.0036	0.4950	± 0.0065		
0.6	0.5970	± 0.0026	0.5921	± 0.0074		
0.7	0.6944	± 0.0065	0.6627	± 0.0288		
0.8	0.7362	± 0.0211	0.7314	± 0.0217		

targeted value. The set in which there is no packing fraction bias ($a = \alpha_{\text{ex}} = 0$) can achieve $\psi_{6,\text{target}}$ over the largest range, followed by the set which biases toward higher packing fractions (a is nonzero). It is important to emphasize that the range of ψ_6 values achievable by the algorithm is affected by the a and α_{ex} parameters and ultimately by system size.

Another important point to note from Table I is the relative accuracy of the algorithm in producing ψ_6 values. Naturally, the parameter set which only fixes $\psi_{6,\text{target}}$ and sets the density controlling parameters to zero demonstrates the greatest accuracy with respect to its ability to reproduce the target value $\psi_{6,\text{target}}$. This is followed by the parameter set with the density-increasing bias in the objective function. The nonzero α_{ex} (density-decreasing bias) has the least accurate targeting ability. This is largely due to the fact that increasing the exclusion angle *completely eliminates* a range of angular positions from consideration, irrespective of their desirability in terms of $\psi_{6,\text{target}}$.

A wide range of densities and degrees of orientational order are accessible using the objective function presented in this work. A plot showing the ensemble averaged packing fraction for various combinations of parameters is presented

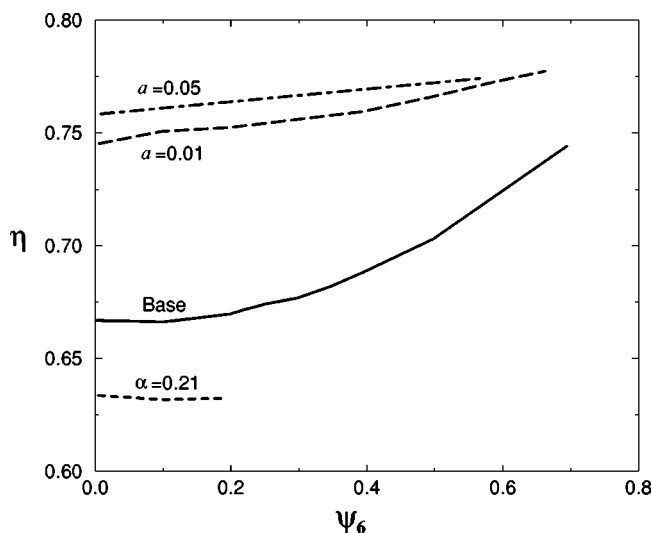


FIG. 3. Plot of density vs actual ψ_6 values for several parameter sets. The set marked “Base” has the parameter set $a = \alpha_{\text{ex}} = 0$. The other sets are labeled by their differences from this set. Results are the average values over between 20 and 100 configurations.

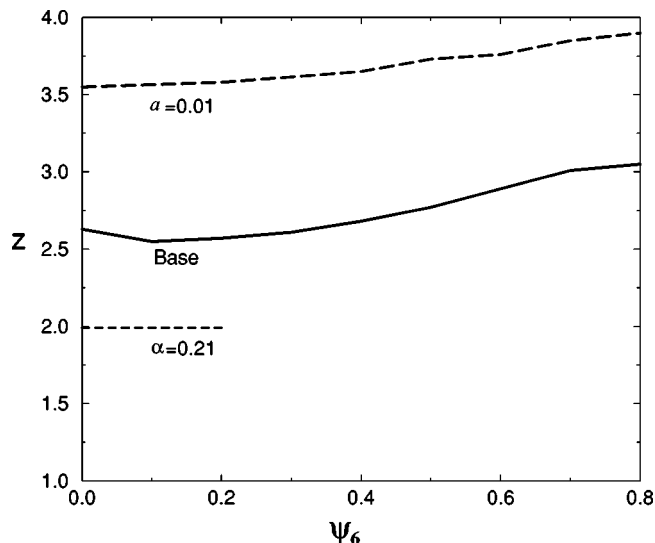


FIG. 4. Plot of mean coordination number vs the actual ψ_6 value for several parameter sets. The base set is $a = \alpha_{\text{ex}} = 0$. The other parameter sets are labeled by their differences from this set.

in Fig. 3. As the figure shows, increasing a has two important effects. First, as a increases, the packing fractions systematically increase. This is to be expected, because this parameter tends to promote the formation of locally compact structures. The densest random configuration ($\eta = 0.763$, $\psi_6 \approx 0$) produced in the $26\sigma \times 26\sigma$ box was achieved by setting $a = 0.2$ (data not shown). A slightly higher packing fraction for a random sample ($\eta = 0.769$) was achieved using the same parameters in a box nine times as large in area, demonstrating minor finite-size effects. In generating dense structures, the algorithm can maintain low values of ψ_6 by preventing the locally ordered regions from aligning. Nevertheless, as a is set to higher values, geometric constraints render this task impossible and $\psi_{6,\text{target}}$ can no longer be matched.

In the parameter range plotted in Fig. 3, there is a limit to the value of ψ_6 that can be attained. This is primarily due to the effect of “temporary” neighbors. Because particles are added in random order, disks that would not be Delaunay neighbors in the final tessellation are neighbors at an intermediate state. These neighbors cause deviations from perfect hexagonal placements, which then propagate to the rest of the system and thwart the growth of locally crystalline structures. It is possible, however, to generate nearly perfect HCP systems by increasing a outside of the range shown above. In particular, a system generated using $a = 1.0$ reproduced a full HCP crystal with as few as five deletion point defects.

As is evident in Fig. 3, increasing α_{ex} decreases the packing fraction attained at a given ψ_6 , while maintaining the network of contacts. This is because a nonzero value for α_{ex} prevents new disks from being placed in gaps where they would have fit for $\alpha_{\text{ex}} = 0$. Thus, the average coordination number z is reduced (Fig. 4), and consequently packing is less efficient. Setting α_{ex} to its maximum value ($\pi/6$) results in a packing fraction of $\eta \approx 0.40$.

We note that the packing fraction in any of the configurations generated using our algorithm can be reduced, with-

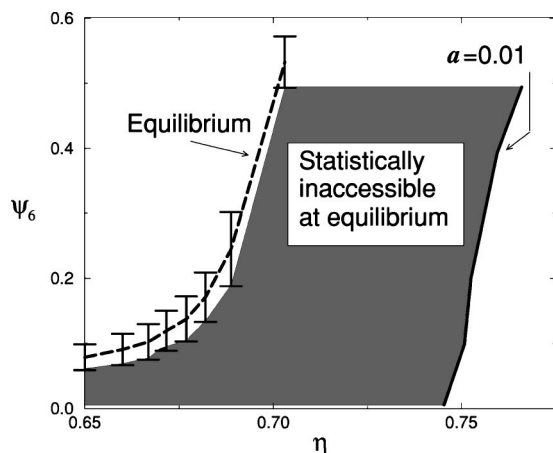


FIG. 5. Comparison between the equilibrium ensemble and configurations generated in the algorithm (using $a=0.01$). The shaded region represent combinations of packing fraction and ψ_6 that are obtainable from the algorithm, but are not statistically significant in the equilibrium ensemble. The equilibrium configurations represent the average of 400 configurations each relaxed through 10^5 Monte Carlo steps. The configurations generated by the algorithm are the same as those illustrated in Fig. 3.

out affecting the orientational order of the system, by decreasing the disk diameters in the final configuration (without displacing their centers), though this destroys the contact network. From this perspective, the curves depicted in Fig. 3 represent *maximum* densities that may be obtained from the methodology presented here.

It is a commonly held notion that the equilibrium fluid samples the most disordered configurations available to it at a given packing fraction. Figure 5 presents a comparison of ψ_6 values between a Monte Carlo equilibrated system and configurations generated by the algorithm, with the parameter $a=0.01$. The shaded region depicts configurations which exhibit coordinate pairs (η, ψ_6) that are not visited with statistical significance in the equilibrium fluid, but in fact can be generated by the seed-growth protocol. Interestingly, we find that *the equilibrium fluid does not sample the most disordered configurations available to it at high density*. In contrast, there is a dramatic increase in orientational order in the equilibrium fluid (relative to the nonequilibrium structures) as the freezing transition ($\eta_f \approx 0.69$) is approached.²⁷

Figure 6 illustrates the radial distribution function $g(r)$ for configurations generated using the parameter sets depicted in Fig. 4. Figure 6(a) corresponds to the set labeled “Base,” $\psi_{6,\text{target}} = a = \alpha_{\text{ex}} = 0$. Figure 6(b) shows the RDF for the set with a high-density bias ($a=0.01$) and Fig. 6(c) the set with a low-density bias ($\alpha_{\text{ex}} = \pi/15$). It is interesting to note that almost no translational order is present at separations larger than 3σ for any of the structures shown. Furthermore, the limitations placed on angular positions when either a or α_{ex} are nonzero produce interesting variations in the translational order within the system. Within the short-range translational order, a few peaks are present for the systems with nonzero a or α_{ex} . The peaks present in Fig. 6(b), are at positions which indicate the presence of small HCP regions. In Fig. 6(c), the large peak at $r/\sigma = 1.166$ is formed by placements in which the bonds connecting two

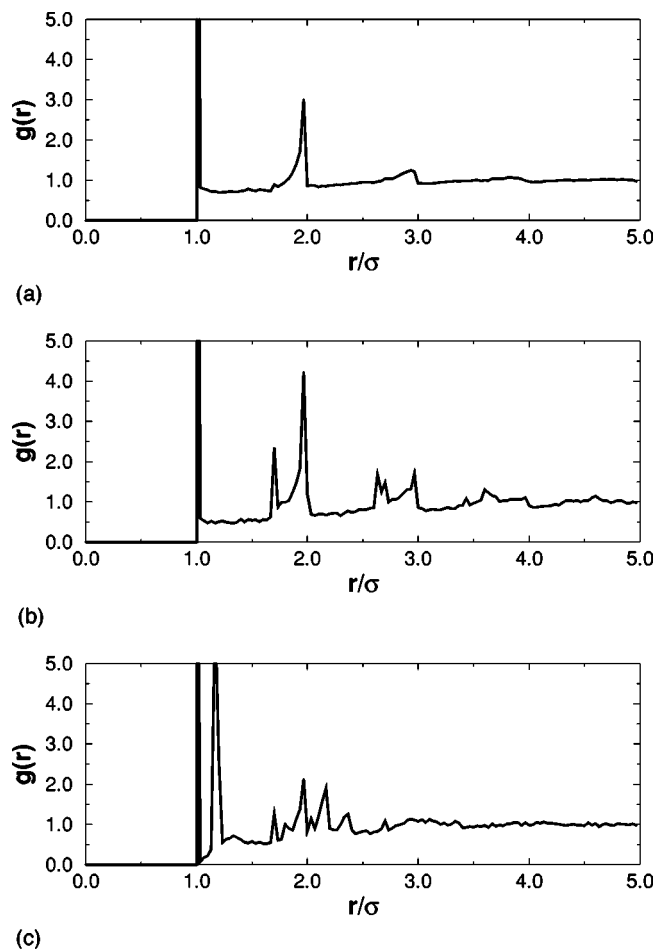


FIG. 6. Radial distribution functions for three parameter sets. A description of the parameter sets used is contained within the text. (a) $\psi_6 = 0.0024$, $\eta = 0.667$; (b) $\psi_6 = 0.0048$, $\eta = 0.745$; (c) $\psi_6 = 0.0045$, $\eta = 0.634$.

disks to a common third disk form an angle of $\pi/15$. Again, this order is strictly of the short-range variety.

In addition, finite-system-size effects have some effect on the packing density of the systems generated here. Because of the periodic boundary conditions, interactions between the surfaces of the growing system come into play. Because the final disks placed are unlikely to fit perfectly between two advancing surfaces, space is wasted and the packing fraction reduced. To estimate the importance of this effect, several configurations were generated for the parameter set $\psi_{6,\text{target}} = a = \alpha_{\text{ex}} = 0$, in systems of varying size. The packing fraction from the smallest system ($26\sigma \times 26\sigma$) is $\eta \approx 0.667$. For a system four times as large in area, the packing fraction increase to $\eta = 0.669$, while at nine times the area the packing fraction reaches $\eta = 0.671$. A simple extrapolation, postulating the form

$$\phi = c + d/(\text{Area}) \quad (9)$$

in which c and d are parameters, leads to an estimated packing fraction of $\eta \approx 0.672$ in the infinite limit. Other parameter sets also suggest that the error in achieving a desired ψ_6 value is reduced as system size increases, but this has yet to be measured systematically.

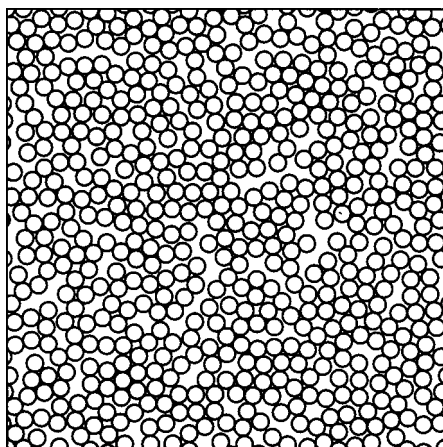


FIG. 7. One realization of the Eden model adapted to the hard-disk system. $\psi_6=0.015$, $\eta=0.677$.

IV. DISCUSSION

An algorithm has been presented that allows nonequilibrium systems of hard disks to be generated with controlled degrees of bond-orientational order. The algorithm begins with a seed of a few disks and adds new disks in a sequential process. Each disk is placed such that it is in contact with at least one previously placed disk. Subject to this constraint, the position which best suits an objective function targeting a specified degree of orientational order is found. The process terminates once no space is available for the placement of any additional disks. This method allows a significant range of orientational order to be explored (from 0 to 0.70 in the base algorithm).

Systems in which a low degree of orientational order is targeted also possess essentially no translational order beyond a few disk diameters. As greater orientational order is demanded, translational order characteristic of hexagonal close packing develops. In addition, two parameters in the algorithm allow for the packing fraction to be biased. Systems with little orientational order ($\psi_6 \sim 0.01$) are attainable with packing fractions as high as $\eta=0.769$. At densities greater than this, significant orientational order appears. However, even at these densities, translational order indicative of the presence of small HCP crystal regions is present.

Systems in which the ψ_6 value is minimized may be considered to be random with respect to orientational order. In evaluating the randomness of these systems, it is useful to compare to a slightly generalized Eden growth model. The original Eden model²⁸ involves the growth of a cluster on a lattice. In the Eden model, an occupied site on the edge of the cluster is chosen randomly and a neighboring empty site is turned occupied. This process can be adapted to the hard-disk system such that a disk at the edge of a cluster is chosen and a neighbor disk is placed in contact with it at some random angular position (which avoids any overlaps). This is equivalent to using the algorithm presented here, but instead of selecting a placement based on the objective function in Eq. (5), the choice of θ is made randomly. As such, configurations generated by this adapted Eden model may be considered perfectly random as defined by ψ_6 . One such real-

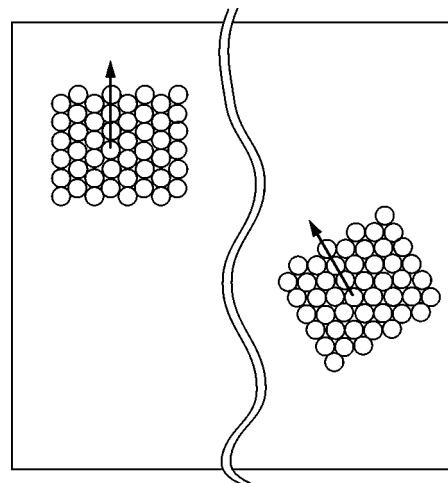


FIG. 8. A system in which ψ_6 is a poor measure of order. The left half of the plane is tiled with a HCP crystal oriented along the arrow. The right half is also tiled with a HCP crystal, which is rotated through an angle of $\pi/6$ relative to the left side. In the infinite size limit this leads to a ψ_6 value of zero.

ization is presented in Fig. 7. Visually, this configuration shows no signs of any orientational order. Averaged over 100 configurations, the Eden model has an average packing fraction of $\eta=0.655$ and an orientation order of $\psi_6=0.037$. Both of these values are comparable to those obtained from the minimized order systems. That the minimized systems display an average ψ_6 value that is somewhat lower than the truly random Eden model should not be taken to indicate that they are more random. Instead, it shows that a very low value of the order parameter ψ_6 serves to indicate randomness, but, since ψ_6 is only a partial measure of bond-orientational order, it is not capable of providing quantitative distinctions at very low values.

An extension to the algorithm, which should allow local HCP regions to be avoided, is the use of an averaged local orientational order in place of the global orientational order. Such a parameter can be defined as

$$\langle \psi_{6,i} \rangle = \frac{1}{N} \sum_j \left| \sum_k e^{6i\theta_{jk}} \right|. \quad (10)$$

The global order parameter suffers from the failing that a configuration in which the majority of the disks are in regions of HCP packing, may still display a low ψ_6 value provided that these regions are not oriented with respect to one another. An extreme case is one in which the entire system consists of two equal sheets of perfect HCP packings (see Fig. 8). If these two sheets are oriented such that one is rotated through an angle of $\pi/6$ relative to the other, the global ψ_6 value will be zero, although it is obvious that the system actually displays substantial orientational order. Naturally, the use of an averaged local orientational order is expected to have some failings as well. For example, it is likely that systems with substantial degrees of global order will be very difficult to generate from the local measurement. Some preliminary work on the use of the average local orientational order parameter has been done and the results support our initial predictions. A sample realization, generated

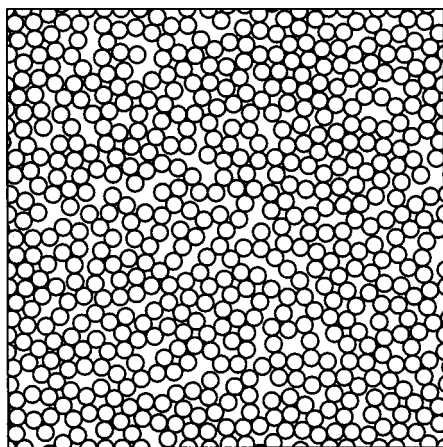


FIG. 9. One realization of an algorithm in which the order parameter defined in Eq. (10) is minimized. $\psi_6=0.029$, $\eta=0.663$, $\langle\psi_{6,i}\rangle=0.294$.

by minimizing the value of $\langle\psi_{6,i}\rangle$, is shown in Fig. 9. Note that the local order parameter $\langle\psi_{6,i}\rangle$ is quite far from zero, leading to the interesting question of whether there is a minimum, nonzero value of this parameter for a random system.

Another interesting possibility is the inclusion of translational freedom in the placement of new disks. This would allow the relation between orientational and translational order to be studied in detail. Work seeking to describe this relation is currently underway,²⁹ but including it in an algorithm such as the one described here might allow the relationship to be specified rather than measured. Such an algorithm would be an important step in understanding the nature of truly random packings and in creating such systems.

ACKNOWLEDGMENTS

S.T. thanks the School of Mathematics at the Institute for Advanced Study for its hospitality during his stay there. He also acknowledges the Guggenheim Foundation for his Guggenheim Fellowship to conduct this work. The work was

also supported by the Engineering Research Program of the Office of Basic Energy Sciences at the Department of Energy (Grant No. DE-FG02-92ER14275). T.M.T. acknowledges the support of the National Science Foundation.

- ¹B. J. Alder and T. E. Wainwright, *J. Chem. Phys.* **33**, 1439 (1960).
- ²F. H. Stillinger, E. A. DiMarzio, and R. L. Kornegay, *J. Chem. Phys.* **40**, 1564 (1964).
- ³B. D. Lubachevsky and F. H. Stillinger, *J. Stat. Phys.* **60**, 561 (1990).
- ⁴B. D. Lubachevsky, F. H. Stillinger, and E. N. Pinson, *J. Stat. Phys.* **64**, 501 (1991).
- ⁵R. J. Speedy, *J. Phys.: Condens. Matter* **10**, 4185 (1998).
- ⁶A. P. Gast and W. B. Russel, *Phys. Today* **51**, 24 (1998).
- ⁷A. Mehta and G. C. Barker, *Phys. Rev. Lett.* **67**, 394 (1991).
- ⁸B. A. Cornell, J. Middlehurst, and N. S. Parker, *J. Colloid Interface Sci.* **81**, 280 (1981).
- ⁹H. Reiss, *J. Phys. Chem.* **96**, 4736 (1992).
- ¹⁰S. Torquato, T. M. Truskett, and P. G. Debenedetti, *Phys. Rev. Lett.* **84**, 2064 (2000).
- ¹¹G. D. Scott and D. M. Kilgour, *Br. J. Appl. Phys.* **2**, 863 (1969).
- ¹²W. M. Visscher, *Nature (London)* **239**, 504 (1972).
- ¹³W. S. Jodrey and E. M. Tory, *Phys. Rev. A* **32**, 2347 (1985).
- ¹⁴D. J. Adams and A. J. Matheson, *J. Chem. Phys.* **56**, 1989 (1972).
- ¹⁵G. D. Scott, *Nature (London)* **194**, 956 (1962).
- ¹⁶J. L. Finney, *Proc. R. Soc. London, Ser. A* **319**, 479 (1970).
- ¹⁷C. H. Bennett, *J. Appl. Phys.* **43**, 2727 (1972).
- ¹⁸A. Z. Zinchenko, *J. Comput. Phys.* **114**, 298 (1994).
- ¹⁹J. M. Kosterlitz and D. J. Thouless, *J. Phys. Chem.* **6**, 1181 (1973).
- ²⁰B. I. Halperin and D. R. Nelson, *Phys. Rev. Lett.* **41**, 121 (1978).
- ²¹D. R. Nelson and B. I. Halperin, *Phys. Rev. B* **19**, 2456 (1979).
- ²²A. P. Young, *Phys. Rev. B* **19**, 1855 (1979).
- ²³A. Okabe, B. Boots, and K. Sugihara, *Spatial Tessellations* (Wiley, New York, 1992).
- ²⁴P. J. Steinhardt, D. R. Nelson, and M. Ronchetti, *Phys. Rev. B* **28**, 784 (1983).
- ²⁵T. I. Quickenden and G. K. Tan, *J. Colloid Interface Sci.* **48**, 382 (1974).
- ²⁶G. C. Barker and A. Mehta, *Phys. Rev. A* **45**, 3435 (1992).
- ²⁷This is consistent with the recent identification of a structural precursor to the freezing transition in the hard-disk system [T. M. Truskett, S. Torquato, S. Sastry, P. G. Debenedetti, and F. H. Stillinger, *Phys. Rev. E* **58**, 3083 (1998)].
- ²⁸M. Eden, in *Proceedings of the 4th Berkeley Symposium on Mathematical Statistics and Probability 4* (University of California Press, Berkeley, CA, 1961).
- ²⁹T. M. Truskett, S. Torquato, and P. G. Debenedetti, *Phys. Rev. E* **62**, 993 (2000).